Hydraulic design and numerical investigation of twin-screw hydraulic turbine for high pressure power recovery

Q. Li[1], S. H. Liu[2], X. P. Jiang[3]*, L. Zhou[3]*, W. Li[3]

[1] *School of Environment and Safety Engineering, Jiangsu University, Zhenjiang, China*
[2] *The Institute of Seawater Desalination and Multipurpose Utilization, SOA, Tianjin, China*
[3] *National Research Center of Pumps, Jiangsu University, Zhenjiang, China*

As a novel type of energy recovery device based on the reverse operation principle of screw pump, the twin-screw turbines (TSHT) are widely used in high-efficiency sea water reverse osmosis systems. It is important to investigate the performance and internal flow patterns of TSHT. The research presents the hydraulic design of TSHT and analyzes the general characteristics of the internal flow field and the efficiency performance by numerical simulation and experimental methods. In order to solve the Navier-Stokes equations for three-dimensional unsteady flow, dynamic mesh technique was used in the commercial Computational Fluid Dynamics (CFD) software. Pressure distribution and velocity distribution, as well as efficiency performance of the flow field were studied by the numerical simulation method which was validated by the prototype experiment. The twin-screw hydraulic turbine (TSHT) can be widely used in sea water reverse osmosis systems for power recovery due to its stable performance.

Key words: Twin-screw turbines, Hydraulic design, CFD, Numerical simulation, Energy recovery

INTRODUCTION

The twin-screw hydraulic turbine (TSHT) is a novel type of energy recovery device based on the reverse operation principle of a screw pump. It can be widely used in petrochemical, electric power, metallurgy, environmental protection, ammonia synthesis, seawater desalination and other industrial processes. The recycling of pressure energy from the high-pressure wastewater in these processes can help reduce carbon emissions and environmental pollution [1-8].

At present, the research on hydraulic turbine is mainly concentrated on the reverse operation of the centrifugal pump used as a hydraulic turbine. Barbarelli *et al*. [9] used a predictive model to predict the performance of the centrifugal pumps used as turbines by a theoretical computation method. Sanjay *et al*. [10] carried out experimental investigations to improve the performance of the pumps as turbines by optimizing its geometric and operational parameters. Yang *et al*. [11,12] predicted the performance of the single-stage centrifugal pumps as turbines based on theories, simulations and experiments, and studied the influence of blade wrap angle and blade inlet angle on the centrifugal pump. Zhu *et al*. [13] also proposed an optimal design method to ensure high efficiency and steady operation of the pump-turbine runner. Despite the research on hydraulic turbines has attained many achievements, most of the pumps

as turbines are not suitable for the small flow rate, high head water and even ultrahigh head water inlet working conditions, except the multistage pump as turbine being able to run under conditions of high inlet pressure but with low efficiency [14,15].

For the screw-type energy recovery device, Tang *et al*. [16] have theoretically and experimentally studied the performance of a twin-screw expander. Kovacevic *et al*. [17] have used the numerical simulation method to study the combined screw compressor-expander machines for use in high pressure refrigeration systems. Papes *et al*. [18] have studied the flow inside a screw expander, which will help in optimization of the screw expander's performance by CFD calculations. In the field of single screw mechanical energy recovery, Waters [19] has put forward the use of Archimedes spiral pump as a turbine. Rohmer *et al*. [20] have analyzed the performance of this model by means of modeling design and experiment. In addition, Xia *et al*. [21] have investigated the performance of a single-screw expander of different inlet vapor dryness, but there are no reports on twin-screw pumps used as turbines.

Twin-screw hydraulic turbine (TSHT) has the advantages of stable medium transport, weak pressure pulsation, low mechanical vibration and noise, simple and compact structure, as well as long serving period. Most importantly, TSHT could handle a gas-liquid two-phase flow. As a volumetric liquid turbine, the efficiency is still an important indicator of its performance. The decrease in efficiency is mainly influenced by the

*To whom all correspondence should be sent:
E-mail: jxp2502@163.com

combination of various gaps in its structure. In this paper, the influence of the general characteristics of the internal flow field and the effect of the leakage on the efficiency of the internal flow field are analyzed by the CFD numerical simulation method.

MATERIALS AND METHODS

Hydraulic design

Twin-screw hydraulic turbine (TSHT) is based on the inverse operation principle of the twin-screw pump. Compared with other pumps as turbines (PAT), TSHT has a relatively compact structure. The entire turbine is split into inlet cavity and outlet cavity by two screws, as shown in Fig. 1. When the working medium flows from the inlet to the inlet cavity, the pressure inside the cavity would continue to rise. Then the working medium flows into the front bushing hole acting on the helicoid surfaces of screws under the inlet cavity pressure. After that, the medium flows through the back bushing hole and outlet cavity and finally flows out of the outlet. The differential pressure in the adjacent screw seal chamber produces a rotational torque to drive the twin screws. The sum of the torques of the main-follower screws can be transmitted by main screws to drive a generator or a power machinery connected with actuator shaft, thus conversing the fluid pressure energy to electricity or mechanical energy and achieving the purpose of energy recovery.

The transmission of the main-follower screws relies on a pair of meshing gears with the same transmission ratio for avoidance of the screw locking caused by small lead. Since the main screw bears the most torque and axial force in most cases, it is used as the actuator shaft. The main screw is also provided with a pair of positioning plates to ensure that it will not cause axial displacement under the action of axial force produced by medium pressure, thus playing a role of positioning and thrusting. The screw profile of type A can in theory divide the inlet cavity and outlet cavity into two connected parts, so as to greatly improve the volumetric efficiency of TSHT. Furthermore, the whole device has the advantages of simple structure and easy processing. The tooth curves of type A twin screw pumps contain four types of basic curves. They are arc, prolate epicycloid, involute, and curtate epicycloid, as shown in Fig. 2 and Table 1. The main size parameters on the main and follower screws are summarized in Table 2.
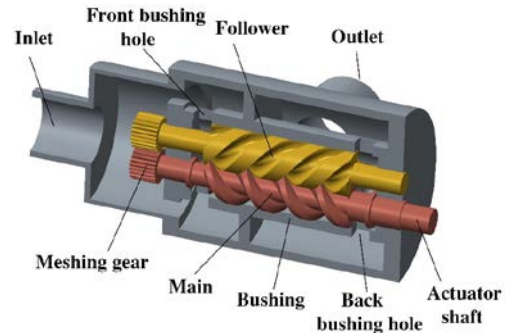

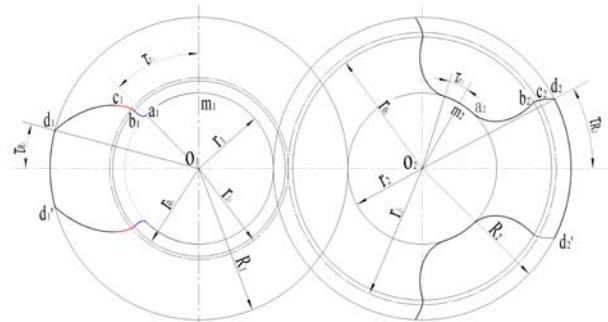**Fig. 1.** Structure of the twin-screw hydraulic turbine

Fig. 2. Tooth curves and basic dimension parameters

Table 1. Geometrical characteristics

Tooth profile curves	Main screw	Tooth profile curves	Follower screw
m_1a_1	Arc (radius=r_1)	m_2a_2	Arc (radius=r_2)
a_1b_1	Prolate epicycloid	a_2b_2	Prolate epicycloid
b_1c_1	Involute	b_2c_2	Involute
c_1d_1	Curtate epicycloid	c_2d_2	Curtate epicycloid
d_1d_1'	Arc (radius=R_1)	d_2d_2'	Arc (radius=R_2)

Table 2. Main size parameters of the main and follower screw

Parameter	Main screw		Follower screw	
	Symbol	Value	Symbol	Value
Gear number	n_1	2	n_2	3
Radius of addendum circle	R_1	31mm	R_2	31mm
Rated axial distance of screws	C	46.5mm	/	/
Meshing angle of involute	α	15°	α	15°
Central angle of addendum circle	τ_{R1}	14.7°	τ_{R2}	30°
Central angle of dedendum circle	τ_{r1}	45°	τ_{r2}	9.8°
Radius of pitch circle	r_{j1}	18.6mm	r_{j2}	27.9mm
Radius of base circle	r_{o1}	17.97mm	r_{o2}	26.95mm
Radius of dedendum circle	r_1	15.5mm	r_2	15.5mm
Coefficient of addendum height	H_1	2/3	H_2	1/9

Calculation domain and meshes

The calculation domain used in this paper is shown in Fig. 3. It is totally based on a real model. The interface is set between the fluid domain of inlet cavity and the fluid domain of screw. The CAD models of inlet and outlet fluid domain are imported into Pumplinx for generation of a cartesian grid. The dynamic mesh technique is used to simulate the flow field changing with time due to the boundary motion.
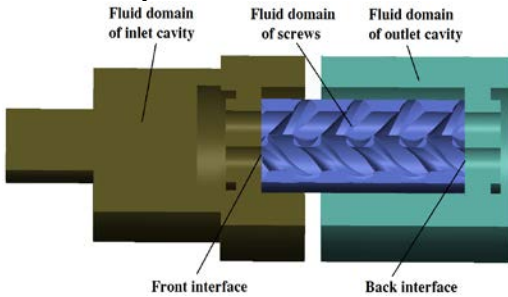

Fig. 3. Calculation domain and interfaces

The mesh of screw fluid domain can keep overall transformation as time step increases, which can be interpreted as a type of re-meshing of overall mesh. However, this type of re-meshing has no restriction on the initial mesh. In the process of pretreatment, a rotation period is divided into several meshing states, with each meshing state corresponding to a fluid domain model in each time step. Fig. 4 presents the overall mesh of the screws fluid domain and the mesh on screw surface.
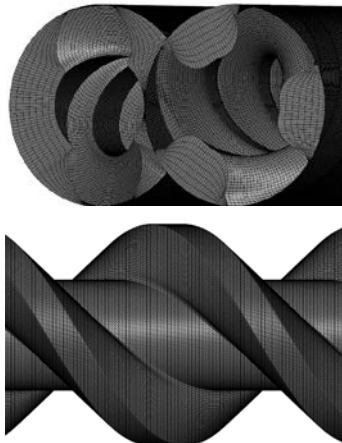

Fig. 4. **Mesh on screw domain and screws surface**

Grid sensitivity analysis

The number of radial grid tiers is one of the important factors that affect the total number of grids and the grid sensitivity. It can significantly affect the value of Y+ and directly relate to the first tier of the grid nodes near the boundary set in the region where the turbulence is fully developed, thus having an impact on simulation. The influence of different radial grid tiers on the simulation results in the fluid domain of screw is studied as shown in Fig. 5. The TSHT with 4-7 radial grid tiers is numerically simulated. The torque, flow rate, and efficiency under the simulated conditions of 1.0MPa inlet pressure, 0.02MPa outlet pressure and the Y+ variation range of the whole flow field under the simulated condition of 0.2-1.0MPa inlet pressure are shown in Table 3.
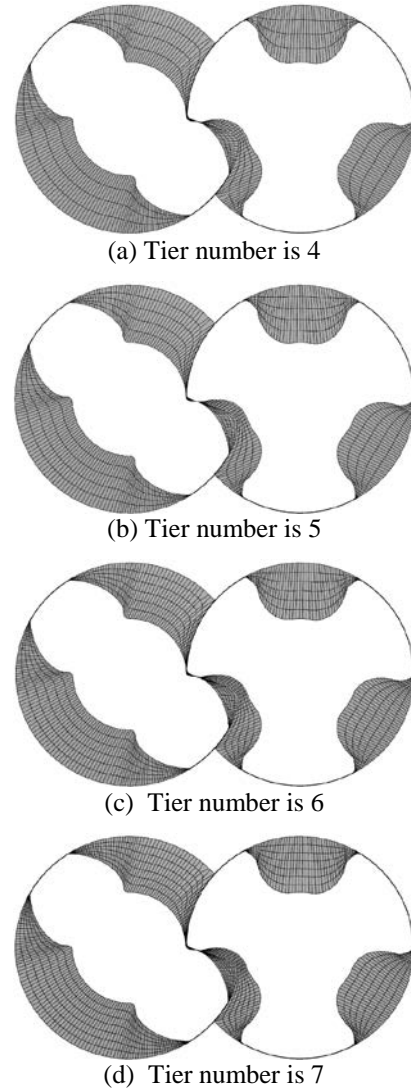

(a) Tier number is 4

(b) Tier number is 5

(c) Tier number is 6

(d) Tier number is 7

Fig. 5. Different tier numbers in radial direction

As shown in Table 3, the torque, flow rate and efficiency do not change significantly as the number of grid tiers increases, which indicates that the influence of the number of grid tiers on the above parameters can be ignored. But considering the rationality of the first tier grid nodes, when radial grid has a tier of 7, the value of Y+ is more reasonable thus making the simulation results more credible. Therefore, the number of radial grid tiers in the screw fluid domain was set to 7.

Table 3. Grid sensitively with different number of tiers

Number of tiers	Torque (N·m)	Flow rate (m³/h)	Efficiency (%)	Y^+
4	24.129	13.527	59.55	74.0~154.8
5	24.141	13.522	59.60	65.7~131.9
6	24.133	13.525	59.57	49.2~108.4
7	24.135	13.528	59.56	35.1~68.5

Turbulence model and boundary

In consideration of the specific conditions of the fluid flow and the flow field characteristics of TSHT, the following assumptions are used: (a) the fluid is incompressible, (b) the flow field is stable and isothermal, (c) the inertia force, and gravity are negligible, (d) the fluid is completely filled in the volume, and (c) the turbine is working at a stable rotating speed.

The flow through the model pump was simulated with the commercial code Pumplinx, which employs the finite volume method to solve the Reynolds averaged Navier-Stokes equations for the 3D incompressible unsteady flow. The CFD flow domain was divided into two types of subdomains. The outlet section belongs to the first type of subdomain, and the equations for this type of region are solved in a stationary framework. The second type of subdomain is the screw passage that simulates the rotating process of the screws by the dynamic mesh technique. The rotational speed was set to 900r/min according to the experimental value. The interfaces were formed between different subdomains. The boundary conditions were set to pressure inlet and pressure outlet by considering the coupling fluctuation with the flow rate. The inlet pressure ranged from 0.2 to 1.8MPa at an interval of 0.2MPa, and the outlet pressure was set to 0.02MPa, approximating the actual conditions.

RESULTS AND DISCUSSION

Experimental validation

The TSHT model used in this paper was established and tested. A high pressure energy recovery test rig was designed and established in the National Research Center of Pumps, China. The schematic arrangement of the test rig facility and test equipment are shown in Figs. 6 and 7, which have the identification from the technology department in Jiangsu province of China.

This test rig was based on an open-type system. A booster pump was driven by a motor with variable-frequency drive (VFD) to adjust the inlet pressure of different values. Pressure sensors were set in both the inlet and outlet of TSHT. A torque-speed sensor was installed on the output shaft to measure the torque and rotation speed. The combination of generator and electrical load was used to consume the power generated by the turbine, and the rotating speed could be controlled by adjusting the electrical load that was placed in a circuit of the generator. In the experiment, both the flow meter and the torque-speed sensor had a precision of 0.5% FS, and the pressure had a precision of 0.1% FS. All sensors and instruments had electrical output signal of 4-20mA. PLC was used in this test rig to achieve automatic control, as illustrated in Figs. 6 and 7 presenting the test rig, including the connection of turbine, torque-speed sensor and generator.
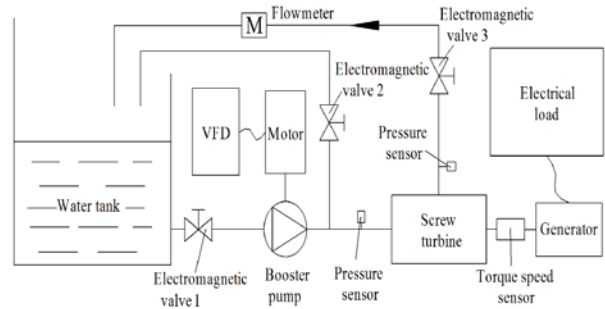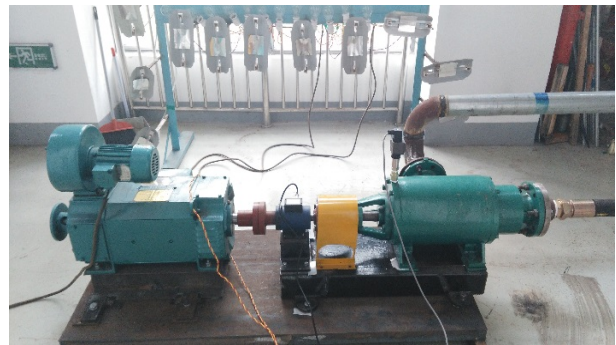

Fig. 6. System diagram of the test rig

Fig. 7. Shaft power load and dissipation module

Fig. 8 presents the comparison between simulation and experimental results. The flow rate and the efficiency obtained by the experiment had the similar varying tendency with that obtained by numerical simulation. However, as the pressure rose, the error between experiment and simulation had an obvious increasing trend. The changing trends were basically the same, indicating that the simulation was consistent with the actual condition. The main reason for the increasing error is that as the inlet pressure rose, the axial force actcng on the screws increased, thus leading to the rise of mechanical losses in the location of bearings, which cannot be predicted by the simulation method in this study. Overall, there was a good agreement between the experiment and simulation results, which could further prove the accuracy of the numerical methods used.
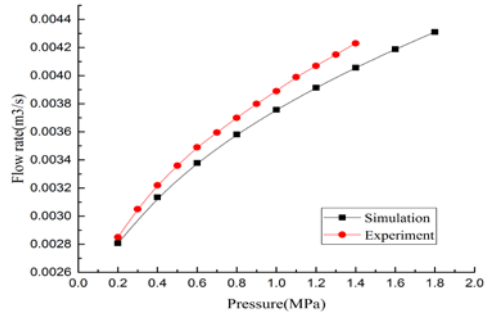
(a) Flow rate
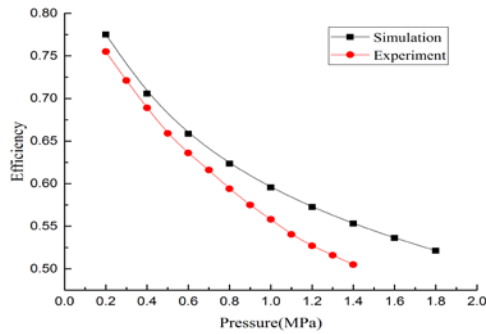
(b) Efficiency

Fig. 8. Comparison of flow rate and efficiency between simulation and experiment

Numerical analysis

In this paper, a CFD numerical simulation analysis was carried out to illustrate the common characteristics of the TSHT under the working conditions of 1.0MPa inlet pressure and 0.02MPa outlet pressure.

The screw surface pressure distribution at a rotating speed of 900r/min is shown in Fig. 9. The inlet cavity and outlet cavity maintained the high and low pressure distribution, respectively. The screw was divided into 5 sealing chambers with different pressure levels in its effective length under the influence of meshing curve sealing function and the third sealing rule. The inlet side of the screw had the highest pressure and the outlet side had the lowest pressure. The distribution of the meshing curve can be clearly seen from the pressure cloud diagram, and it had the same distribution characteristics as the pressure level boundary of the different seal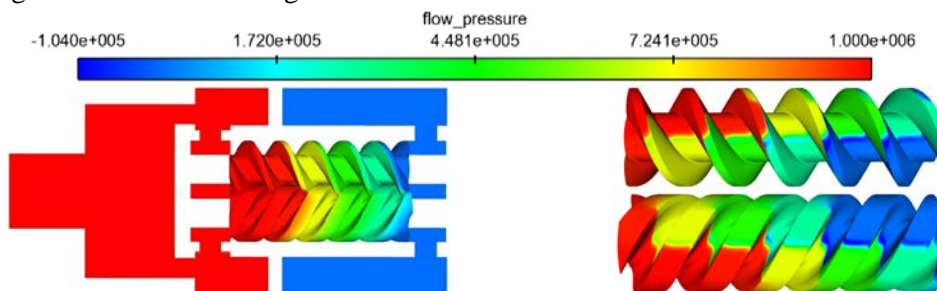ing chambers. The sealing chambers at the same pressure level were connected under the current meshing condition. In addition, near the meshing curve there would be low pressure area or even negative pressure area relative to the sealing chamber on both sides of the meshing curve. The reason for this is that the medium in leakage clearance near the meshing curve has a higher leakage flow rate. Based on the principle of energy conservation, the pressure will be relatively lower.

Fig. 10 shows the velocity distribution of TSHT. First of all, for twin screws in a meshing state, the screw dedendum circle surface relative to the outer spiral tooth surface and addendum circle surface have a relatively low surface velocity distribution, especially for follower screw with a lower dedendum surface velocity. From the velocity vector diagram sectioned along the screw middle section we can see that the working medium that flows in or out of the screw fluid domain through the bushing hole maintains a relatively low flow velocity (kinetic energy). The flow velocity of the medium keeps rising as it gradually flows into the screw seal chamber till acting on the screw spiral surface. Then some of the medium flows into the radial clearance and produces jet-flow of higher velocity. Jet-flow in the first radial clearance from the inlet side of screw is not very obvious. While from the second radial clearance it maintains the basic characteristics of a high-speed jet-flow.

The flow velocity distribution in the central section of the screws is shown in Fig. 11, where the left is the inlet side of the screw and the right is the outlet side. It can be clearly seen that the leakage flow rate in the flank clearance has several rules of changing: high-speed flow occurs in the minimum flank clearance, and as the flow area in the clearance is reduced, the velocity has a trend of rapid rising. The site with the minimum flank clearance is the place where the meshing point is located. And because of the sealing effect of the meshing line, the two sides of the meshing point show different levels of pressure.
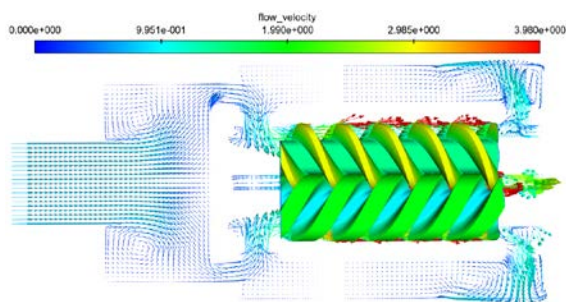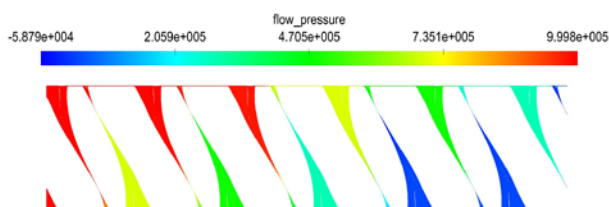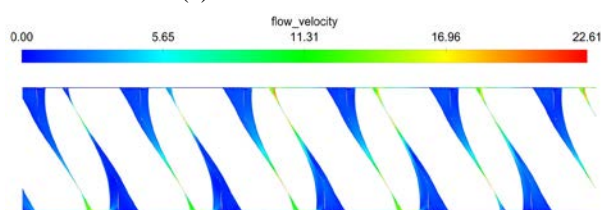

Fig. 9. Pressure distribution

Fig. 10. Velocity distribution diagram

(a) Pressure distribution

(b) Velocity distribution

Fig. 11. Gear side clearance leakage pressure and velocity distribution

CONCLUSIONS

(1) The adjacent screw teeth form a multistage seal cavity. Each stage seal cavity divided by meshing curve has different pressure levels while the sealing chambers in a connected state without the sealing action of meshing curve have the same pressure level. The pressure near the inlet of the sealing cavity is the highest one while the pressure near the outlet is the lowest one; the distribution of the meshing curve and the demarcation line of different pressure levels have the same distribution characteristics. In addition, in the leakage clearance near the meshing curve, low pressure area, or even the negative pressure area will appear relative to the sealing cavity on both sides of the meshing curve. This is the result of the transformation of pressure energy into kinetic energy.

(2) The twin-screw dedendum circle surface in a meshing state has a relatively low surface velocity distribution and the flow velocity gradually increases as the medium gradually enters the screw sealing cavity until it acts on the screw spiral surface. Due to the pressure difference between the adjacent sealing cavities, some medium will enter the radial clearance and produce a jet-flow with higher velocity. The inlet and outlet of the radial clearance have a certain length of convergence and jet segments. The velocity of flow shows a sharp rising trend with the decrease of flank clearance.

The interlobe clearance has a higher leakage velocity.

REFERENCES

1. W. Liu, L. Henrik, V.M. Brianet, X. Zhang, *Applied Energy*, **88**, 518 (2011).
2. L. Francis, *Energy Policy*, **35**, 2187 (2007).
3. X.H. Wang, J.H. Yang, F.X. Shi, *Journal of Drainage and Irrigation Machinery Engineering,* **09**, 742 (2014).
4. H.L. Huang, Z. Yan, *Renewable and Sustainable Energy Reviews*, **13**, 1652 (2009).
5. Varun, R. Prakash, I.K. Bhat, *Renewable and Sustainable Energy Reviews,* **13**, 2716 (2009).
6. B. Orchard, S. Klos, *World Pumps*, **8**, 22 (2009).
7. L. Yao, B. Liu, Z.X. Wu, *Nuclear Engineering and Design,* **237**, 1468 (2007).
8. W.A. Raja, R.W. Piazza, *Desalination*, **38**, 123 (1981).
9. S. Barbarelli, M. Amelio, G. Florio, *Energy*, **107**, 103(2016).
10. V. J. Sanjay, S. Abhishek, H. M. Karan, N. P. Rajesh, *Energy Conversion and Management*, **89**, 808 (2015).
11. S. S. Yang, D. Shahram, F. Y. Kong, *Renewable Energy,* **48**, 507 (2012).
12. S. S. Yang, F. Y. Kong, H. Chen, X. H. Su, *ASME Journal of Fluids Engineering*, **134**, 061102 (2012).
13. B.S. Zhu, X.H. Wang, L. Tan, D.Y. Zhou, Y. Zhao, S.L. Cao, *Renewable Energy*, **81**, 366 (2015).
14. P. Francesco, D.P. Francesco, F. Nicola, G. Maurizio, M. Gustavo, *Renewable Energy*, **99**, 180 (2016).
15. Z.G. Zuo, S.H. Liu, Y.K. Sun, Y.L. Wu, *Renewable and Sustainable Energy Reviews*, **41**, 965 (2015).
16. H. Tang, H.G. Wu, X.L. Wang, Z.W. Xing, *Energy*, **90**, 631 (2015).
17. *K. Ahmed, S. Nikola, I.K. Smith, Simulation Modelling Practice and Theory*, **14**, 1143 (2006).
18. I. Papes, J. Degroote, J. Vierendeels, *Applied Thermal Engineering*, **91**, 535 (2015).
19. S. Waters, G.A. Aggidis, *Renewable and Sustainable Energy Reviews,* **51**, 497 (2015).
20. J. Rohmer, D. Knittel, G. Sturtzer, D. Flieller, J. Renaud, *Renewable Energy*, **94**, 136 (2016).
21. G. D. Xia, Y. Q. Zhang, Y. T. Wu, C. F. Ma, W. N. Ji, S. W. Liu, H. Guo. *Applied Thermal Engineering*, **87**, 34 (2015).